Chapter 3
Infrared Spectroscopy in Studying Biofunctionalised Gold Nanoparticles

Alexander A. Kamnev

Abbreviations

ATR	Attenuated total reflectance
DRIFT	Diffuse reflectance infrared fourier transform
FGNP	Functionalised gold nanoparticles
FTIR	Fourier transform infrared
GlcNAc	*N*-acetyl-D-glucosamine
$(GlcNAc)_3$	N', N'', N'''-triacetylchitotriose
GOX	Glucose oxidase
hIgG	Human immunoglobulin
IR	Infrared
SEIRA	Surface-enhanced infrared absorption
TEM	Transmission electron microscopy
WGA	Wheat germ agglutinin

3.1 Introduction

Over the last decade, nano-sized particles of noble metals with surface plasmon-resonance properties have found numerous applications in nanotechnology and scientific research, including diverse biological and biomedical fields (for recent reviews see, e.g. [1–9]. This also refers to (bio) functionalised metal nanoparticles, where the term "functionalisation" (or "biofunctionalisation") means conjugation of metal nanoparticles via either covalent bonds (e.g. involving thiol groups easily forming –S–metal bonds) or non-covalent binding forces (adsorption via charge attraction and/or hydrophobic interactions) with specific types of molecules [5, 10–12].

A. A. Kamnev (✉)
Laboratory of Biochemistry, Institute of Biochemistry and Physiology of Plants and Microorganisms, Russian Academy of Sciences, Prospekt Entuziastov 13, Saratov, Russia, 410049
e-mail: aakamnev@ibppm.sgu.ru; a.a.kamnev@mail.ru

O. Fesenko et al. (eds.), *Nanomaterials Imaging Techniques, Surface Studies, and Applications*, Springer Proceedings in Physics 146,
DOI: 10.1007/978-1-4614-7675-7_3,

The latter include, in particular, recognising bio(macro)molecules, such as antibodies, lectins, enzymes, peptide aptamers or nucleic acid aptamers, etc. [3], which are capable of participating in various biospecific interactions of the type "recognising molecule—target molecule". These types of biofunctionalised noble-metal nanoparticles can be useful in revealing such biospecific interactions with the relevant target molecules with a high sensitivity. In such cases either the noble-metal nanoparticles *per se* play the role of a direct "visualising agent" (in microscopic methods) or their surface plasmon-resonance properties are made use of (in optical and spectroscopic techniques).

To understand in detail the properties, stability and behaviour of these sophisticated metal nanoparticle–biomacromolecule conjugate systems [5, 13–15] and, also very importantly, to control their synthesis as well as to explore and develop proper useful applications [3, 16–18], various experimental methods and modern instrumental techniques are absolutely necessary [6, 19]. Among the latter, a range of molecular spectroscopy techniques has been successfully used [20], including UV–Vis spectrophotometry and vibrational [mainly Raman scattering and Fourier transform infrared (FTIR)] spectroscopy.

Spectrophotometry, largely in the visible region and, occasionally, in the near-IR, is useful for controlling the shape, size and aggregation of metal nanoparticles [21–25]. This is due to their typical extinction bands in the characteristic regions of plasmon resonance, both the position (wavelength in the maximum) and intensity of which are sensitive to the aforementioned characteristics of metal nanostructures. Thus, UV–Vis spectrophotometry is often used as a supplementary technique for the characterisation and/or monitoring of nanoparticle-based systems in suspensions and some of the processes occurring therein.

Vibrational spectroscopic techniques are of great importance both in the characterisation of functionalised metal nanoparticles (this refers primarily to their 'outer functional shells' of biomolecules which give specific vibrational patterns, depending on the state of their functional groups as well as on selective 'surface enhancement' effects) and in their diverse bioanalytical applications (for general reviews see, e.g. [26–28]). In particular, for functionalised metal nanoparticles the 'surface enhancement' effects and surface selection rules play a significant role in increasing the spectral sensitivity.

It is well known that in surface-enhanced Raman scattering (SERS) spectroscopy (for reviews on SERS see, e.g. [27, 29–31]), the enhancement factors reaching 10^{10}–10^{12} (up to 10^{15} for a combination of electromagnetic, resonance and chemical enhancements at 'hot spots') are much greater than those in surface-enhanced IR absorption (SEIRA) spectroscopy (for reviews on SEIRA see, e.g. [27, 32–34]). In SEIRA, the enhancement factors can reach values of the orders of 10^{2}–10^{3} at best, while more usually they are of the order of units or tens [28, 35]. Owing to that, SEIRA spectroscopy is far less developed, studied and, consequently, less frequently used, being virtually "the neglected child of surface enhanced spectroscopies" [28]. Nevertheless, the cross-section values in infrared absorption are significantly higher than those in Raman scattering, so that the overall average sensitivities in SEIRA and SERS may be well comparable [33].

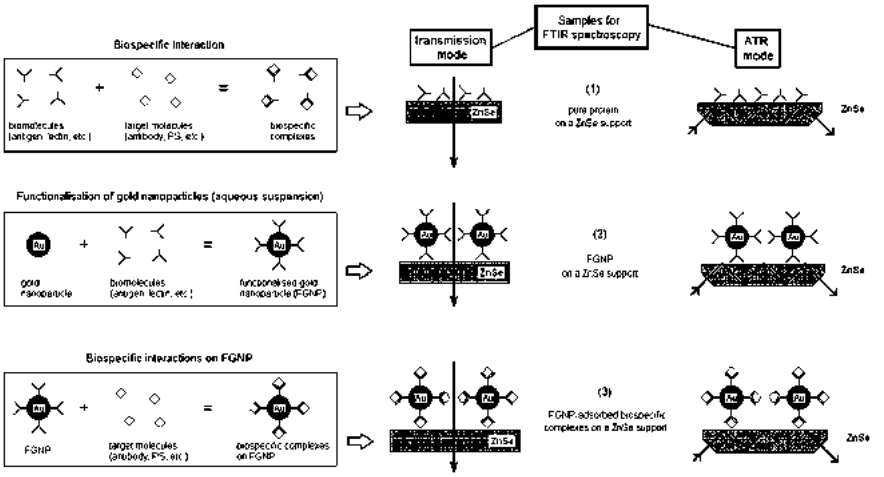

Fig. 3.1 Schematic presentation of the processes of biospecific interactions between pure biomolecules in solution (*upper left-hand panel*), functionalisation of gold nanoparticles by biomacromolecules (*middle left-hand panel*) and biospecific interactions on functionalised gold nanoparticles (FGNP; *lower left-hand panel*), as well as of the corresponding samples for FTIR spectroscopic measurements in the transmission or ATR modes on ZnSe supports (*right-hand panels* 1–3, respectively)

In addition, as a 'useful' supplement (partly compensating for the drawback of the strong water absorption in the infrared), FTIR/SEIRA spectra may give a wealth of complementary information as compared with Raman/SERS spectra.

In this chapter, some representative examples are reviewed and discussed in which Fourier transform infrared (FTIR) spectroscopy in various modes (transmission, diffuse reflectance (DRIFT), attenuated total reflectance (ATR) [36]) was applied for studying biofunctionalised gold nanoparticles, as well as for the detection and analysis of relevant biospecific interactions of the type "recognising molecule—target molecule" (e.g., using antigen–antibody or lectin–carbohydrate biospecifically interacting pairs) at the molecular level, where one type of the molecules from a pair was conjugated with gold nanoparticles (Fig. 3.1). The experimental results considered herein illustrate some possibilities of FTIR/SEIRA spectroscopy complementary to those discussed in previous reviews on its applications in biological or biomedical fields [28, 33–35, 37].

3.2 FTIR Spectroscopy in Studying Gold Nanoparticles Functionalised by Biomacromolecules

Virtually, the only significant intrinsic drawback of IR spectroscopy, as compared with Raman scattering, consists in a very strong IR absorption of water in several regions related to its O–H stretching and different bending vibrations. This fact is

of utmost importance, especially in biological and biomedical studies. Thus, if a biological sample contains a substantial amount of water (or is studied wet, which is sometimes practised for tissues and cells or even for biomacromolecules), in order to obtain reliable spectroscopic data, the spectral contribution of water must be carefully and fully compensated by its removal from the resulting IR spectrum (e.g. by quantitatively subtracting the spectrum of water obtained from a similar adequate "blank reference" sample). This is often a very challenging task, and it may also be additionally complicated by multiple hydrogen bonding in which water is readily involved. What is even more important, different types of such hydrogen bonding can significantly (and, quantitatively, almost always unpredictably) alter not only the intrinsic vibration frequencies of water contained in the sample in an appreciable proportion, but also those of the functional groups of the sample which are involved in the H-bonding. An alternative way of avoiding water-induced 'spectroscopic artefacts' while using 'wet' samples in FTIR spectroscopic studies implies the analysis of FTIR absorption regions or selected bands not overlapping with the typical water absorption regions.

In an earlier paper devoted to the development of SEIRA-based immunoassays [38], silicon plates were used sputter-coated with a very thin ($\sim$10 nm) gold film. Onto the film, either of the two proteins, glucose oxidase (GOX) or antibodies to glucose oxidase (anti-GOX), was immobilised, and FTIR/SEIRA spectra were compared for the immobilised protein and after its biospecific interaction with the other one. Whatever the results, it has to be noted that damp samples (immediately after their removal from the aqueous solutions) were used for measuring FTIR spectra. Thus, it could be seen that the strong and broad water absorption, particularly in the region at $\sim$1,650 cm^{-1}, completely masked the typical amide I ($\sim$1,650 cm^{-1}) and amide II ($\sim$1,540 cm^{-1}) bands of the proteins, so that other regions, with a few weak bands, were analysed [38].

In the next report from virtually the same group [39], goat anti-GOX immunoglobulin (IgG) and a few other immunoglobulins were conjugated with gold nanoparticles (10 nm average diameter), the conjugates were collected by vacuum filtering through porous Qualitative Polyethylene Infrared Cards (3M), and each of their FTIR/SEIRA spectra was measured also on such a wet porous polyethylene 3M IR card. The amide I band of any of the IgG proteins used (at $\sim$1,650 cm^{-1}) could also not be observed in that case owing to the presence of liquid water on the surface. However, it was specially mentioned [39] that the amide II region at $\sim$1,540 cm^{-1}, which was outside the water band absorption, was still not observed in the spectrum of the antibodies. (We would like to note here that a well-resolved amide II band at 1,540 cm^{-1} yet appeared in the SEIRA spectrum of the colloidal gold/anti-GOX/GOX complex on a similar wet 3M IR card [39], i.e. after the biospecific interaction of nanoparticle-conjugated GOX with anti-GOX; see our discussion below in Sect. 3.3).

The absence of the typical amide II band in FTIR/SEIRA spectra of a protein (IgG conjugated with gold nanoparticles), despite its being outside the water band absorption, was intriguing. In order to check whether it was still the effect of water or of the gold nanoparticle surface, a study was undertaken using ATR-FTIR

(SEIRA) spectroscopy of dried films of 30 nm-diameter gold nanosphere–protein conjugates [40].

The ATR-FTIR spectrum of pure staphylococcal protein A (shown in Fig. 3.2a), widely used in immunoassays [41], represented characteristic IR absorption regions of proteins, including the stretching modes of amide N–H at 3,290 and 3,077 cm^{-1} (on the background of a very broad absorption of carboxylic and alcoholic O–H groups in side chains centred at about 3,400 cm^{-1}); symmetric and antisymmetric vibration bands of CH_2 and CH_3 groups of amino acid side chains (within 3,000–2,800 cm^{-1}); strong typical amide I and amide II bands (representing mainly the stretching C=O and bending N–H modes of peptide moieties, respectively, at 1,652 and 1,540 cm^{-1}); bending CH_2 modes at 1,453 cm^{-1}; stretching C–NH_2 of side-chain primary amines near 1,400 cm^{-1}, as well as various weaker bands related to C–N, C–O and C–C–O vibrations of the protein backbone and amino acid residues under 1,350 cm^{-1} [36, 38–40, 42].

Interestingly, the spectrum of protein A conjugated with CG (shown in Fig. 3.2b) was found to be essentially different from that of pure protein A (cf. Fig. 3.2a). First of all, it should be noted that the amount of protein A in the sample of its CG conjugate taken for ATR-FTIR measurement (see Fig. 3.2b) was approximately fivefold less than that of pure protein A (see Fig. 3.2a). Nevertheless, the two to threefold higher absorbance values in maxima in Fig. 3.2b as compared to those in Fig. 3.2a indicate that a SEIRA effect was observed with enhancement factors of the order of 10–15. These values correspond largely to the electrostatic and hydrophobic nature of the gold nanoparticle surface conjugation with a biospecific probe due to the net effect of relatively weak non-covalent interactions, which allows the nativity of biomacromolecules and their functional

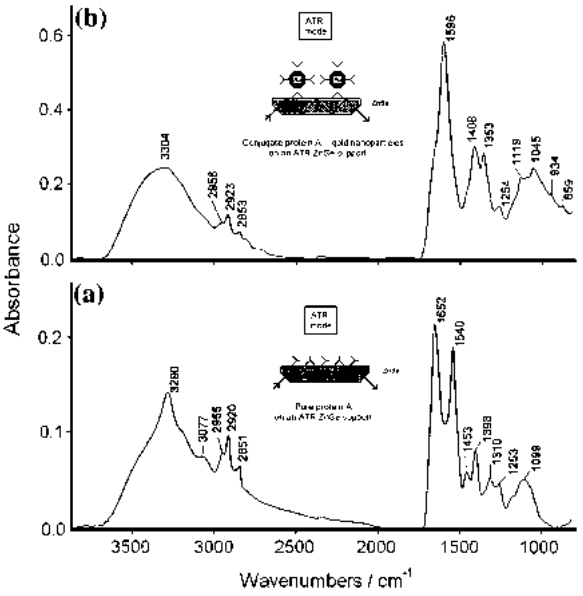

Fig. 3.2 ATR-FTIR spectra of dry films of staphylococcal protein A: (**a**) pure (100 μg of protein), (**b**) conjugated with colloidal gold (20 μg of protein; schemes of the samples are shown above each spectrum). All spectra were measured on a standard ZnSe 45° flat-plate ATR contact sampler (12 reflections). Redrawn using some data from [40] to illustrate information presented therein

activity to be conserved (see [40] and references reported therein). It is known that stronger chemical (covalent) interactions of adsorbed molecules with the metal surface can result in enhancement factors increased by over one order of magnitude [32].

Second, the SEIRA spectrum (see Fig. 3.2b) showed that the amide N–H band at 3,290 cm^{-1} (see Fig. 3.2a) virtually disappeared. Moreover, instead of the amide I (1,652 cm^{-1}) and amide II (1,540 cm^{-1}) bands, in the SEIRA spectrum of the dry film of the gold nanoparticle–protein A conjugate there appeared a single intermediate strong peak centred at 1,596 cm^{-1} (with a shoulder at about 1,650 cm^{-1}). These changes may indicate that N–H moieties of the protein are directly involved in its interaction with the metal surface. Also enhanced are the regions of C–NH_2 vibrations near 1,400 cm^{-1} (see Fig. 3.2b), suggesting the involvement of side chain amino groups, and of C–C/C–O vibrations (1,150–1,000 cm^{-1}). Note that according to the SEIRA theory [32], only those molecular vibrations which appear perpendicular to the metal surface are enhanced, accounting for the selectivity of enhancement.

Thus, the ATR-FTIR/SEIRA result obtained using the dried film of the gold nanoparticle–protein A conjugate (see Fig. 3.2b; [40]) accounts for the absence of amide II band in the SEIRA spectra of wet colloidal gold conjugates with immunoglobulins discussed above [39]. In addition, the drastic changes in the spectrum of protein A induced by gold nanoparticles upon conjugation can provide evidence that protein molecules are attached directly to the gold nanoparticle surface, which is of primary importance for the synthesis of haptens with colloidal gold for subsequent immunisation of animals [43]. Thus, the FTIR-SEIRA methodology may be used for controlling the bioconjugation process [40].

It may be reasoned that, upon protein conjugation with the surface of a nanoparticle, the protein conformation may undergo some changes. It is important to emphasise that, if so, this could only partly, but certainly not fully, account for the observed FTIR (SEIRA) spectroscopic changes, since the latter are expected to be induced largely by the specific and selective surface enhancement of certain functional groups most close to the gold surface, considering also the surface selection rules for their vibrations [32]. For instance, conformational changes in bovine serum albumin (BSA) upon its conjugation with gold nanospheres (18 $\pm$ 2 nm in diameter) were also suggested [44] on the basis of comparative Raman scattering and SERS spectroscopic data. Note that the S–S stretching vibration of disulphide bridges observed in Raman spectra of BSA at 515 cm^{-1} was also observed in the SERS spectrum of BSA conjugate (with a slight shift to 520 cm^{-1}) with a comparable intensity [44]. This result showed that the disulphide bonds in BSA molecules remained largely unbroken upon BSA adsorption onto the 18 nm gold nanospheres.

On the other hand, there is a noteworthy report [45] where BSA was used for functionalisation of very small gold nanoparticles (less than 2 nm in diameter). For the resulting conjugate, the involvement of –S–Au protein–nanoparticle covalent bonds was proven by Raman spectroscopy (the S–S stretching mode of disulphide bonds in BSA reported to be at 508 cm^{-1} was found to completely disappear upon

BSA conjugation with the nanoparticles) and confirmed by calculations from energy-dispersive X-ray spectra (EDS). As a result, the FTIR spectra of pristine BSA and of the BSA–nanoparticle conjugate (both measured in dry powder pellets pressed with KBr) were found to be essentially similar, including the typical amide I (at 1,653 cm^{-1}) and amide II ($\sim$1,550 cm^{-1}) bands. This may be attributed to the absence of noticeable conformational changes of the protein backbone upon conjugation with such small nanoparticles. Last but not least, such small gold nanoparticles (<2 nm) are characterised by the absence of surface plasmon resonance owing to quantum size effects [45, 46] and, hence, lack of any selective surface enhancement (SEIRA) effects which could affect the FTIR spectrum of the conjugated protein.

A similar virtually undisturbed FTIR spectrum of pepsin (with the typical amide I band at 1,648 cm^{-1} and amide II at 1,536 cm^{-1}) was observed for a drop-dried pepsin conjugate with small gold nanoparticles (3.5 nm in diameter) on a Si(111) substrate measured in the diffuse reflectance (DRIFT) mode [47]. In that case, however, a weak broad feature at 2,520 cm^{-1} (typical of the –S–H stretching vibrations of cysteine residues in pepsin) was observed also in the conjugate, showing that not all of the cysteine residues were bound to the gold surface. Nevertheless, in that case 3.5 nm Au nanoparticles still exhibited a plasmon resonance band, which was reported to be initially at 512 nm and, for the conjugate in aqueous suspension (at pH $\sim$3 common for pepsin), was observed in UV–Vis spectra as a broadened peak at higher wavelengths (between 500 and 600 nm) together with the absorbance at 280 nm (π–π* transitions of the tryptophan and tyrosine residues in conjugated pepsin).

The FTIR spectroscopic data discussed above imply that in certain cases, e.g. when the size of the gold nanoparticles used for conjugation with a protein is relatively small (a few nm), the FTIR spectra of the pristine protein and of the protein attached to the gold nanoparticles may well show similar patterns (with much smaller differences than those seen in Fig. 3.2a, b, particularly in the amide I and amide II regions within $\sim$1,700–1,500 cm^{-1}). Of course, this spectroscopic similarity would be additionally facilitated when the small Au nanoparticles lack surface plasmon resonance owing to quantum size effects, so that no bands of the gold-conjugated protein could be selectively surface-enhanced.

It may also be suggested that, when a protein is bound to the gold nanoparticle surface largely by a number of covalent –S–Au bonds (rather than by non-covalent bonds via adsorption), its FTIR spectrum may well be generally similar to that of the pristine protein, showing only slight changes (e.g. in the secondary and/or tertiary structure). For example, in a recent paper [48], transforming growth factor-beta 1 (TGF-β1) was shown to conjugate to gold nanospheres ($\sim$13 nm in average diameter) via S–Au bonds. High-resolution X-ray photoelectron spectroscopy data for the TGF-β1–Au conjugate showed that 70.2 % of the three-component sulphur signal (S 2p) were due to S–Au bonds (the component at 162.1 eV), with the remaining 17.3 % of free thiol groups (S–H, 163.2 eV) and 12.5 % of disulphide (S–S, 163.8 eV), while pristine TGF-β1 contains only disulphide bonds in its dimeric molecule [48]. In the FTIR spectra (measured in the reflection mode from

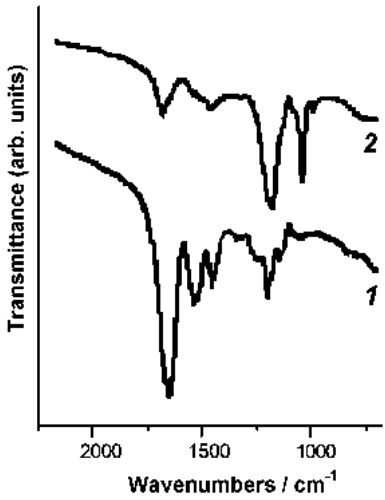

Fig. 3.3 FTIR spectra of free A3 dodecapeptide (*1*) and A3 conjugated with gold nanoparticles (*2*). Redrawn using some data from [49] (Supporting Information) to illustrate information presented therein

dry films on an Al plate), both the amide I and amide II bands were well resolved, while the comparative analysis of the amide I band profiles showed substantial conformational changes of TGF-β1 upon conjugation (note that the quantitative data for the secondary structure components in pristine TGF-β1 were found to be close to those for the NMR structure of solution-form TGF-β1 in the Protein Data Bank).

Yet, in many cases, FTIR data reported in the literature provide evidence for noticeable changes, involving both the band positions and redistribution of intensities, observed in FTIR spectra of proteins upon their adsorption onto gold nanoparticles or gold films. This may be illustrated by marked spectroscopic changes exhibited by an oligopeptide upon adsorption on gold nanoparticles. The A3 dodecapeptide (AYSSGAPPMPPF, where A = alanine, Y = tyrosine, S = serine, G = glycine, P = proline, M = methionine, F = phenylalanine) contains amino acids capable of interacting with the Au surface via non-covalent bonds. Its conjugate with gold nanospheres ($\sim 13 \pm 3$ nm in diameter determined by TEM) showed a FTIR spectrum (measured from a film on a Si wafer) which significantly differed from that of pure A3 [49] both in band positions and in redistribution of intensities (Fig. 3.3).

3.3 FTIR Spectroscopy in Studying Biospecific Interactions Involving Biofunctionalised Gold Nanoparticles

3.3.1 Immunochemical Interactions

It is well known that biomacromolecules which can be involved in biospecific interactions of the type "recognising molecule—target molecule", when conjugated with gold nanoparticles, particularly via non-covalent bonding, most often

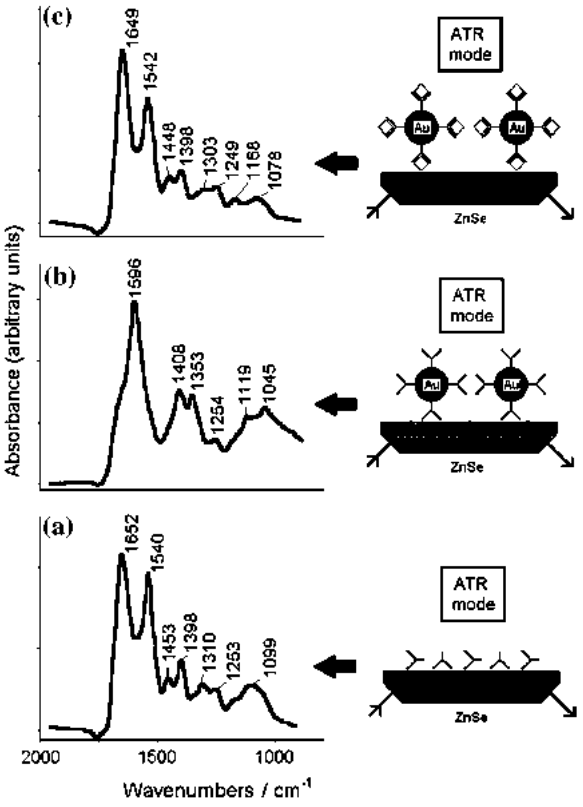

Fig. 3.4 ATR-FTIR spectra (in the region under 2,000 cm^{-1}) of dried films of (**a**) pure protein A (100 μg of protein), (**b**) protein A conjugated with 30 nm gold nanospheres (20 μg of protein), (**c**) the same as (**b**) after interaction with hIgG in aqueous solution (schemes of the samples are shown on the right-hand panels). All spectra were measured on a standard ZnSe 45° flat-plate ATR contact sampler (12 reflections). Redrawn using some data from [51] to illustrate information presented therein

retain their binding capability, which is used in various assays involving colloidal gold bioconjugates [3]. In view of that, considering also the FTIR/SEIRA spectroscopic changes observed upon functionalisation of gold nanoparticles by biomacromolecules (see Sect. 3.2 and Fig. 3.2), it was of interest to study the FTIR spectroscopic behaviour of the biospecifically interacting pair.

With regard to the biospecifically interacting pair protein A—immunoglobulin, an important effect was observed after the immunochemical interaction of the gold nanospheres/protein A complex with human immunoglobulin (hIgG) in solution [40]. When the gold nanoparticles functionalised by protein A (antigen) were mixed in aqueous suspension with traces of hIgG (antibody) dissolved in water (see Fig. 3.1, lower left-hand panel), the resulting biospecific complex on gold nanoparticles (see Fig. 3.1, lower right-hand panel, sample 3) exhibited further FTIR spectroscopic alterations, in particular, in the amide I–amide II regions ($\sim$1,700–1,500 cm^{-1}).

In Fig. 3.4, FTIR-ATR spectra (in the most informative region under 2,000 cm^{-1}) of dried films on a ZnSe support are shown for pure protein A (spectrum *a*) as well as its conjugate with 30 nm gold nanospheres before (spectrum *b*) and after biospecific interaction with hIgG (spectrum *c*). The spectroscopic

changes observed in going from spectrum *b* to spectrum *c* consist in the 'restoration' of the main shape of the initial spectrum of protein A (see spectrum *a*), in particular, the well-resolved amide I and amide II bands, with a ca. 15-fold enhancement; the latter is somewhat smaller only in the C–C–O spectral region (1,150–1,000 cm^{-1}). This finding accounts for the appearance of the amide II band observed after immunochemical interaction of gold nanoparticle-conjugated GOX with anti-GOX on wet 3M IR cards, while the amide I band was still 'obscured' by water absorption near 1,650 cm^{-1} [39], as discussed above in Sect. 3.2.

This result makes it possible to detect such immunochemical interactions using the SEIRA effect with an enhancement factor found to be 10–15 [40], typical for SEIRA of adsorbed biomolecules. Importantly, the addition of BSA, which does not react with protein A, as a control to the colloidal gold/protein A complex had no effect on its spectrum.

In is important to emphasise that the spectrum of pure hIgG (reported also for comparison by [40], although generally resembling that of protein A (see Fig. 3.2a), was shown to have some essential differences. The fact that spectrum c in Fig. 3.4 (for the gold nanoparticle/protein A/hIgG complex) largely coincides in shape with that of pure protein A (see spectrum *a*) and differs from that of the gold nanoparticle/protein A complex (see spectrum *b*, Fig. 3.4) suggests that upon the reaction of hIgG with protein A on the surface of gold nanoparticles, the configuration of protein A is modified. This is in line with the observations obtained earlier using SERS spectroscopy for another immune reaction on colloidal gold [50]. Moreover, it is unlikely that hIgG bound to protein A on gold nanoparticles as an 'outer shell' (i.e. additionally separated from the CG surface; see Fig. 3.1, lower right panel, sample 3) would exhibit any comparable SEIRA effect.

Note also that smaller gold nanoparticles (e.g., 15 nm in diameter) are more stable in solution and, although giving a somewhat less clear-cut FTIR-SEIRA spectroscopic changes than those observed on 30 nm particles (see [51] and references reported therein), can also be used for the SEIRA spectroscopic detection of biospecific interactions.

3.3.2 Lectin–Carbohydrate Interactions

A similar approach was attempted for FTIR spectroscopic investigation of lectin–carbohydrate interactions [51, 52]. It should be mentioned that there are relatively few reports related to lectin–carbohydrate specific biosensors (see, e.g. [53–56], and references therein).

A plant lectin, wheat germ agglutinin (WGA), was used for functionalising gold nanoparticles [52]. Wheat lectin (WGA) has been reported to induce multiple metabolic effects in wheat-associated rhizobacteria under appropriate conditions (see [51, 57], and references reported therein). The development of such effects is commonly initiated by biospecific interactions in a pair "receptor molecule—target molecule". In particular, WGA is well known to specifically bind *N*-acetyl-

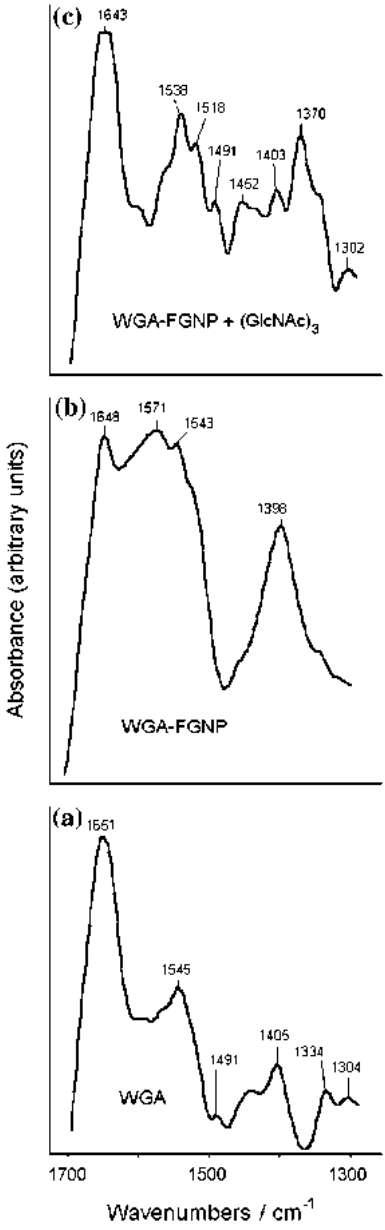

Fig. 3.5 FTIR spectra of dried films of (**a**) pure wheat germ agglutinin (WGA; ca. 20 μg), (**b**) its conjugate with 15 nm gold nanoparticles (ca. 10 μg of WGA), as well as (**c**) the same as (**b**) after interaction with 5 μg $(GlcNAc)_3$ in aqueous solution. All spectra were measured in the transmission geometry on standard ZnSe crystal discs (Ø 13 mm, 2 mm thick). Redrawn using some data from [51, 52] to illustrate information presented therein

D-glucosamine (GlcNAc) residues (see, e.g. [58], which are present in some bacterial cell-surface biomacromolecules, thus bringing about the aforementioned multiple metabolic effects in bacterial cells under appropriate conditions.

Gold nanospheres (mean diameter 15 nm) functionalised by WGA were found to give SEIRA spectroscopic changes, as compared to pure WGA (cf. Fig. 3.5a, b),

similar to those for the protein A–gold nanoparticle system (see Fig. 3.4a, b). For WGA, the region of amide I and amide II bands is represented by maxima at 1,651 and 1,545 cm^{-1}, respectively, in agreement with the FTIR data reported earlier [58].

In the FTIR absorption spectrum of the dried film of the WGA-gold nanoparticle conjugate (Fig. 3.5b), instead of typical well-resolved amide I and amide II bands, there is an intermediate strong band centred at 1,571 cm^{-1} superimposed on the amide I and II band residues. In addition, there appears a strong band at 1,398 cm^{-1}. These changes, although less clear-cut than in FTIR-ATR spectra of 30 nm gold nanoparticles (see Fig. 3.4), are analogous to those observed in the FTIR spectrum of protein A conjugate with gold nanospheres measured in the transmission geometry [59]. These changes reflect the interactions of amide moieties and amino groups with the gold nanoparticle surface, in agreement with the conclusions drawn by other authors (see above; [51] and references therein). Note that proteins adsorbing onto the gold nanoparticle surface have been shown [60] to displace citrate ions weakly bound at colloidal gold particles formed upon reduction of $[AuCl_4]^-$ ions by citrate. The SEIRA enhancement factors for the WGA-gold nanoparticle system (Fig. 3.5b) were estimated to be also around 10–20 for different bands [52], depending on the orientations of transition dipole moment (TDM) components relative to the metal surface.

After biospecific interactions of the WGA-gold nanoparticle system in aqueous suspension with the GlcNAc trimer, $(GlcNAc)_3$ (N′, N″, N‴-triacetylchitotriose), further IR spectroscopic changes are observed (Fig. 3.5c). In particular, separate amide I and amide II bands have restored, in line with the spectroscopic changes observed for the protein A–hIgG system (cf. Fig. 3.4b, c). As mentioned above, such changes imply that upon biospecific interactions of the proteins with their target molecules, the configuration of the protein attached to the gold surface is modified. This conclusion is in agreement with the observations reported earlier for an immune reaction on colloidal gold using SERS spectroscopy [50]. It was also shown using FTIR spectroscopy [58] that WGA interaction with GlcNAc oligomers as well as with GlcNAc-bearing liposomes is accompanied by conformational changes in the lectin molecules reflected, in particular, in the amide I band profile.

Thus, the FTIR-SEIRA spectroscopic methodology has been shown to be applicable to the detection of lectin–carbohydrate biospecific interactions, using the example of WGA-gold nanospheres interacting with GlcNAc-containing haptens [52] and also with GlcNAc-containing bacterial cell-surface macromolecules [61], in line with their involvement in plant-bacterial interactions via WGA-mediated signalling.

3.4 Conclusions and Outlook

Applications of modern FTIR spectroscopy (in different modes) in biological fields continue to grow, and this is a logical consequence of its versatility, sensitivity, informativity and non-destructive nature. Nevertheless, as has been shown by

several examples in this chapter, further development of FTIR methodology in nanobiotechnology and nanobiosensing is very promising. This concerns not only structural studies of nanomaterials, but also sensitive monitoring of the bioconjugation processes involving metal nanostructures, resulting in their biofunctionalisation. A separate important field relates to further exploiting the surface plasmon resonance properties of biofunctionalised metal nanoparticles and their surface enhancement effects, in particular, SEIRA in FTIR spectroscopy, which has so far been underestimated. Finally, the possibilities for a sensitive detection of various biospecific interactions using FTIR/SEIRA spectroscopy on gold nanoparticles, illustrated in this chapter, should be further developed for a range of nanoparticles of different metals, shapes, sizes and functionalising bio(macro)molecules.

Acknowledgments The author is grateful to Dr. Lev A. Dykman (Saratov, Russia), Prof. P. A. Tarantilis and Prof. M. G. Polissiou (Athens, Greece) for long-lasting collaboration and many stimulating discussions on various methodological aspects related to biofunctionalised gold nanoparticles and, in particular, FTIR spectroscopy applied to their study. Experimental studies of the author considered in this chapter were supported in part by NATO Grants LST.CLG.977664, LST.NR.CLG.981092 and ESP.NR.NRCLG 982857.

References

1. Khlebtsov NG, Dykman LA (2010) Optical properties and biomedical applications of plasmonic nanoparticles. J Quant Spectrosc Radiat Transfer 111:1–35
2. Dykman LA, Khlebtsov NG (2011) Gold nanoparticles in biology and medicine: recent advances and prospects. Acta Naturae 3(2):34–55
3. Dykman LA, Khlebtsov NG (2012) Gold nanoparticles in biomedical applications: recent advances and perspectives. Chem Soc Rev 41(6):2256–2282
4. Hartland GV, Schatz G (2011) Virtual issue: plasmon resonances—a physical chemistry perspective. J Phys Chem C 115:15121–15123
5. Mahmoudi M, Lynch I, Ejtehadi MR, Monopoli MP, Bombelli FB, Laurent S (2011) Protein–nanoparticle interactions: opportunities and challenges. Chem Rev 111:5610–5637
6. Pérez-López B, Merkoçi A (2011) Nanoparticles for the development of improved (bio) sensing systems. Anal Bioanal Chem 399(4):1577–1590
7. Hamad-Schifferli K (2013) How can we exploit the protein corona? Nanomedicine 8(1):1–3
8. Omidfar K, Khorsand F, Azizi MD (2013) New analytical applications of gold nanoparticles as label in antibody based sensors. Biosens Bioelectron 43:336–347
9. Ravindran A, Chandran P, Khan SS (2013) Biofunctionalized silver nanoparticles: advances and prospects. Colloids surfaces B: Biointerfaces. doi:10.1016/j.colsurfb.2012.07.036)
10. You C–C, Chompoosor A, Rotello VM (2007) The biomacromolecule-nanoparticle interface. Nano Today 2(3):34–43
11. Thanh NTK, Green LAW (2010) Functionalisation of nanoparticles for biomedical applications. Nano Today 5(3):213–230
12. Feng J, Pandey RB, Berry RJ, Farmer BL, Naik RR, Heinz H (2011) Adsorption mechanism of single amino acid and surfactant molecules to Au 111 surfaces in aqueous solution: design rules for metal-binding molecules. Soft Matter 7(5):2113–2120
13. Roach P, Farrar D, Perry CC (2005) Interpretation of protein adsorption: surface-induced conformational changes. J Amer Chem Soc 127(22):8168–8173

14. Teichroeb JH, McVeigh PZ, Forrest JA (2009) Influence of nanoparticle size on the pH-dependent structure of adsorbed proteins studied with quantitative localized surface plasmon spectroscopy. Eur Phys J E 30(2):157–164
15. Shemetov AA, Nabiev I, Sukhanova A (2012) Molecular interaction of proteins and peptides with nanoparticles. ACS Nano 6(6):4585–4602
16. Rosi NL, Mirkin CA (2005) Nanostructures in biodiagnostics. Chem Rev 105(4):1547–1562
17. Dykman LA, Bogatyrev VA (2007) Gold nanoparticles: preparation, functionalisation and applications in biochemistry and immunochemistry. Russ Chem Rev 76(2):181–194
18. Gagner JE, Shrivastava S, Qian X, Dordick JS, Siegel RW (2012) Engineering nanomaterials for biomedical applications requires understanding the nano-bio interface: a perspective. J Phys Chem Lett 3(21):3149–3158
19. Gadogbe M, Ansar SM, He G, Collier WE, Rodriguez J, Liu D, Chu I-W, Zhang D (2013) Determination of colloidal gold nanoparticle surface areas, concentrations, and sizes through quantitative ligand adsorption. Anal Bioanal Chem 405(1):413–422
20. Daniel M-C, Astruc D (2004) Gold nanoparticles: assembly, supramolecular chemistry, quantum-size-related properties, and applications toward biology, catalysis, and nanotechnology. Chem Rev 104(1):293–346
21. Khlebtsov NG, Bogatyrev VA, Dykman LA, Melnikov AG (1996) Spectral extinction of colloidal gold and its biospecific conjugates. J Coll Interface Sci 180(2):436–445
22. Shipway AN, Lahav M, Gabai R, Willner I (2000) Investigations into the electrostatically induced aggregation of Au nanoparticles. Langmuir 16(23):8789–8795
23. Kelly KL, Coronado E, Zhao LL, Schatz GC (2003) The optical properties of metal nanoparticles: the influence of size, shape, and dielectric environment. J Phys Chem B 107(3):668–677
24. Willets KA, Van Duyne RP (2006) Localized surface plasmon resonance spectroscopy and sensing. Annu Rev Phys Chem 58:267–297
25. Amendola V, Meneghetti V (2009) Size evaluation of gold nanoparticles by UV − vis spectroscopy. J Phys Chem C 113(11):4277–4285
26. Dovbeshko GI, Fesenko OM, Shirshov YuM, Chegel VI (2004) The enhancement of optical processes near rough surface of metals. Semicond Phys Quant Electron Optoelectron 7(4):411–424
27. Aroca R (2006) Surface-enhanced vibrational spectroscopy. Wiley, Chichester, p 400
28. Larmour IA, Graham D (2011) Surface enhanced optical spectroscopies for bioanalysis. Analyst 136(19):3831–3853
29. Kneipp K, Kneipp H, Itzkan I, Dasari RR, Feld MS (1999) Ultrasensitive chemical analysis by Raman spectroscopy. Chem Rev 99(10):2957–2975
30. Talley CE, Huser T, Hollars CW, Jusinski L, Laurence T, Lane S (2005) Nanoparticle based surface-enhanced Raman spectroscopy. In: Wilson BC, Tuchin VV, Tanev S (eds) Advances in Biophotonics (NATO science series, I: life and behavioural sciences, vol 369, pp 182–195
31. Hering K, Cialla D, Ackermann K, Dörfer T, Möller R, Schneidewind H, Mattheis R, Fritzsche W, Rösch P, Popp J (2008) SERS: a versatile tool in chemical and biochemical diagnostics. Anal Bioanal Chem 390(1):113–124
32. Osawa M (2001) Surface-enhanced infrared absorption. In Kawata S (ed) Near-field optics and surface plasmon polaritons. Topics in applied physics, vol 81, Springer, Berlin, pp 163–187
33. Aroca RF, Ross DJ, Domingo C (2004) Surface-enhanced infrared spectroscopy. Appl Spectrosc 58(11):324A–338A
34. Ataka K, Heberle J (2007) Biochemical applications of surface-enhanced infrared absorption spectroscopy. Anal Bioanal Chem 388(1):47–54
35. Donaldson PM, Hamm P (2013) Gold nanoparticle capping layers: Structure, dynamics, and surface enhancement measured using 2D-IR spectroscopy. Angew Chem Int Ed 52:634–638
36. Schmitt J, Flemming H-C (1998) FTIR-spectroscopy in microbial and material analysis. Int Biodeterior Biodegrad 41(1):1–11

37. Dubois J, Shaw RA (2004) IR spectroscopy. Clinical and diagnostic applications. Anal Chem 76(19):361A–367A
38. Brown CW, Li Y, Seelenbinder JA, Pivarnik P, Rand AG, Letcher SV, Gregory OJ, Platek MJ (1998) Immunoassays based on surface-enhanced infrared absorption spectroscopy. Anal Chem 70(14):2991–2996
39. Seelenbinder JA, Brown CW, Pivarnik P, Rand AG (1999) Colloidal gold filtrates as metal substrates for surface-enhanced infrared absorption spectroscopy. Anal Chem 71(10):1963–1966
40. Kamnev AA, Dykman LA, Tarantilis PA, Polissiou MG (2002) Spectroimmunochemistry using colloidal gold bioconjugates. Biosci Rep 22(5–6):541–547
41. Dykman LA, Bogatyrev VA (1997) Colloidal gold in solid-phase assays. A review. Biochem (Moscow) 62(4):350–356
42. Wanzenbök HD, Mizaikoff B, Weissenbacher N, Kellner R (1997) Multiple internal reflection in surface enhanced infrared absorption spectroscopy (SEIRA) and its significance for various analyte groups. J Mol Struct 410–411:535–538
43. Dykman LA, Matora LYu, Bogatyrev VA (1996) Use of colloidal gold to obtain antibiotin antibodies. J Microbiol Meth 24(3):247–248
44. Iosin M, Toderas F, Baldeck PL, Astilean S (2009) Study of protein–gold nanoparticle conjugates by fluorescence and surface-enhanced Raman scattering. J Mol Struct 924–926:196–200
45. Burt JL, Gutiérrez-Wing C, Miki-Yoshida M, José-Yacamán M (2004) Noble-metal nanoparticles directly conjugated to globular proteins. Langmuir 20(26):11778–11783
46. Alvarez MM, Khoury JT, Schaaff TG, Shafigullin MN, Vezmar I, Whetten RL (1997) Optical absorption spectra of nanocrystal gold molecules. J Phys Chem B 101(19):3706–3712
47. Gole A, Dash C, Ramakrishnan V, Sainkar SR, Mandale AB, Rao M, Sastry M (2001) Pepsin-gold colloid conjugates: preparation, characterization, and enzymatic activity. Langmuir 17(5):1674–1679
48. Tsai Y-S, Chen Y-H, Cheng P-C, Tsai H-T, Shiau A-L, Tzai T-S, Wu C-L (2013) TGF-β1 conjugated to gold nanoparticles results in protein conformational changes and attenuates the biological function. Small. doi:10.1002/smll.201202755
49. Slocik JM, Stone MO, Naik RR (2005) Synthesis of gold nanoparticles using multifunctional peptides. Small 1(11):1048–1052
50. Dou X, Yamaguchi Y, Yamamoto H, Doi S, Ozaki Y (1998) NIR SERS detection of immune reaction on gold colloid particles without bound/free antigen separation. J Raman Spectrosc 29(8):739–742
51. Kamnev AA (2008) FTIR spectroscopic studies of bacterial cellular responses to environmental factors, plant-bacterial interactions and signalling. Spectrosc Int J 22(2–3):83–95
52. Kamnev AA, Dykman LA, Bogatyrev VA, Sadovnikova JN, Tarantilis PA, Polissiou MG (2007) Infrared spectroscopic detection of biospecific interactions using gold nanoparticles functionalised by biomacromolecules. In: Shtykov SN (ed) Proceedings of 10th Analytical Russian-German-Ukrainian symposium (ARGUS'2007—Nanoanalytics), Nauchnaya Kniga, Saratov (Russia), pp 10–13
53. Sadik OA, Yan F (2007) Electrochemical biosensors for monitoring the recognition of glycoprotein–lectin interactions. Anal Chim Acta 588(2):292–296
54. Lyu Y-K, Lim K-R, Lee BY, Kim KS, Lee W-Y (2008) Microgravimetric lectin biosensor based on signal amplification using carbohydrate-stabilized gold nanoparticles. Chem Comm 39:4771–4773
55. Peiris D, Markiv A, Dwek M (2011) A physiological approach to assess the affinity of lectin carbohydrate interactions using cancer cells immobilised on a biosensor surface. Glycobiology 21(11):1523
56. Gorityala BK, Lu Z, Leow ML, Ma J, Liu X-W (2012) Design of a "turn-off/turn-on" biosensor: Understanding carbohydrate-lectin interactions for use in noncovalent drug delivery. J Amer Chem Soc 134(37):15229–15232

57. Kamnev AA, Sadovnikova JN, Tarantilis PA, Polissiou MG, Antonyuk LP (2008) Responses of *Azospirillum brasilense* to nitrogen deficiency and to wheat lectin: a diffuse reflectance infrared Fourier transform (DRIFT) spectroscopic study. Microb Ecol 56(4):615–624
58. Bonnin S, Besson F, Gelhausen M, Chierici S, Roux B (1999) A FTIR spectroscopy evidence of the interactions between wheat germ agglutinin and *N*-acetylglucosamine residues. FEBS Lett 456(3):361–364
59. Kamnev AA, Dykman LA, Tarantilis PA, Polissiou MG (2002) Surface-enhanced Fourier transform infrared spectroscopy of protein a conjugated with colloidal gold. In: Khassanova L, Collery P, Maymard I, Khassanova Z, Etienne J-C (eds) Metal Ions in biology and medicine, vol 7. John Libbey Eurotext, Paris, pp 104–107
60. Chithrani BD, Ghazani AA, Chan WCW (2006) Determining the size and shape dependence of gold nanoparticle uptake into mammalian cells. Nano Lett 6(4):662–668
61. Kamnev AA, Dykman LA, Antonyuk LP, P.A. Tarantilis PA, Polissiou MG (2006) FTIR spectroscopic detection and study of biospecific interactions using functionalised gold nanoparticles. In: Akyüz S, Akalin E (eds) XXVIII European congress on molecular. spectroscopy, Sept 3–8, 2006, Istanbul, Turkey. Book of abstracts, Abstr. No. OA-07, p 31